ACS OMEGA

http://pubs.acs.org/journal/acsodf

Article

Fourier Transform Infrared Spectroscopy for Assessing Structural and Enzymatic Reactivity Changes Induced during Feather Hydrolysis

Xinhua Windt, Elinor L. Scott, Thorsten Seeger, Oliver Schneider, Akbar Asadi Tashvigh, and Johannes H. Bitter*

Cite This: *ACS Omega* 2022, 7, 39924−39930

Read Online

ACCESS | Metrics & More | Article Recommendations | Supporting Information

ABSTRACT: Chicken feathers are major byproducts of the livestock processing industry with high potential in the feed sector. In this study, we present a new approach using Fourier transform infrared (FTIR) spectroscopy to detect the structural changes of feather keratin and its availability for enzymatic hydrolysis (AEH) induced by the thermal pressure hydrolysis (TPH) process. Compared to time-consuming in vitro measurement techniques, the proposed method provides rapid information about the structural changes during TPH which enables quick adaptation of TPH conditions as the quality of the incoming feather changes. By analyzing the FTIR spectra of raw and processed feathers, it was found that AEH negatively relates to the β-sheet content (represented by two IR peaks centered at 1635 and 1689 cm^{-1}), while it positively relates to a new series of peaks centered around 1700 cm^{-1} appearing after the TPH process. The proposed FTIR technique provides a reliable and rapid approach to determine the digestibility indicated by AEH of the processed feather and may be used in process control and optimization.

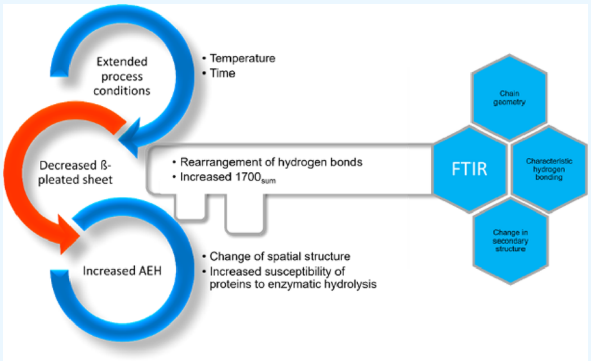

INTRODUCTION

Feathers are a valuable, though challenging, protein-rich feed ingredient. Annually, about 1 million tons of feathers are produced in Europe.[1] Besides their abundant availability, feathers are valuable as a protein feed source as they have a >85% protein content,[2] of which more than 7% is nutritious cystine.[3] However, feathers in their native state have a low nutritional value;[4] they show low availability for enzymatic hydrolysis (AEH) and can hardly be digested by animals.[4,5] This low AEH is caused by their complex stable molecular structure due to the high percentage of stable β-pleated sheets (β-sheet, more than 70%)[6,7] and the presence of strong disulfide bonds,[2] both of which contribute to stable feather keratins. Feathers are made of ß-keratin, a fibrous protein with mainly ß-sheets and a small amount of α-helices and other components in their secondary structure.[8] The ß-sheet consists of laterally packed ß-strands held by hydrogen bonds.[8]

To increase AEH, feathers have to be processed. The molecular structure has to be converted to smaller digestible proteins. Some industrial-scale processes have already been developed:[9] thermal pressure hydrolysis (TPH)[10] optionally in combination with extrusion,[11] chemical hydrolysis,[12] or enzymatic/fermented hydrolysis.[13,14]

TPH is the most common industrial method currently in use. Earlier work has described the effect of temperature (120−160 °C) and time (10 and 30 min) during TPH on AEH,[15] showing four different "stages" characterized by the temperature. The AEH of the hydrolyzed keratin changed at different rates at each stage; however, little is known about the structural changes.

Currently, chemical methods such as ileal digestibility analysis are applied to quantify the AEH.[16] However, it often takes several days to get the final result. Due to the frequently changing raw material quality, which is typical in the rendering industry, it is challenging to get a stable product quality in the real production. Therefore, it is important to detect the quality at an early stage in order to adjust the process conditions. Thus, it is crucial to develop more rapid and facile methods to quantify the AEH content.

Fourier transform infrared (FTIR) spectroscopy as a fast method could be a good alternative to qualify AEH and to guide feather production based on AEH. FTIR spectroscopy is an established tool to study the material stability, reaction mechanism, and kinetics during heat treatment.[17,18] FTIR

Received: July 5, 2022
Accepted: September 28, 2022
Published: October 25, 2022

spectroscopy is often applied to study the secondary protein structure.[19−21] Güler et al. monitored the enzymatically induced degradation of bovine serum albumin using FTIR spectroscopy.[22] Yu et al. studied the secondary structure of feather keratins using synchrotron-based FTIR (S-FTIR) microspectroscopy and stated that S-FTIR spectroscopy is a suitable technique to identify changes in the secondary structure of feed proteins.[23] Cardamone investigated the microstructural change of hydrolyzed keratin extracted from wool and reported that hydrolyzed wool keratin had a similar chemical composition and secondary structure (mainly α-helix) to those of the original untreated wool keratin.[24] Takahashi et al. studied the thermal stability of keratin from defatted and ethanol-treated fowl feathers using differential scanning calorimetry and FTIR spectroscopy. They found that feathers are more stable under dry conditions than under wet conditions.[25]

The secondary protein structure is reflected by IR spectroscopy as bands in the 1700−1600 cm^{-1} (amide I) and 1600−1500 cm^{-1} (amide II) ranges.[26] Amide I is more commonly used to study the protein secondary structure than amide II due to the distribution of vibrations. Amide I represents mainly C═O stretching vibrations (about 80%) and C−N stretching (about 10%) as well as N−H bending (about 10%), whereas amide II contains 60% N−H bending—making it much less "pure".[27]

Besides the application of FTIR spectroscopy for the protein structure, IR technology shows potential in terms of real-time quality monitoring and guiding production.[28−30]

Therefore, the objective of this study is to use FTIR spectroscopy to systematically establish the changes in the secondary structure of feathers (with a focus on the ß-sheet structure) after varying temperatures during TPH and its influence on AEH. We hypothesize that AEH negatively relates to the β-sheet content, while it positively relates to a new series of peaks from 2000 to 1700 cm^{-1}. The heat treatment during TPH causes a rearrangement of hydrogen bonds in the protein structure, that is, opens the ß-sheet structure.[22,31,32] The opened ß-sheet structure releases amino acids for enzymatic hydrolysis which results in the change of AEH. The area from 1700 to 2000 cm^{-1} is the destination of the rearranged hydrogen bonds. A consequence of the structural change is that the protecting spatial structure is opened, thereby making amino acids accessible for enzyme digestion.

2. MATERIALS AND METHODS

2.1. Raw Material and Feedstock Preparation. Chicken feathers (containing 0.4−0.8 wt % ash and 3−5 w % fat, both based on dry matter) were collected from a poultry slaughterhouse within 4 h after plucking. The feathers were transported to the laboratory at 7 °C within 8 h. The feathers were then separated from nonfeather materials, manually mixed thoroughly in order to get a homogeneous mass, washed with tap water, dried at 60 °C overnight until a constant weight was reached, finely chopped and sieved (<1 mm) using a cutting mill (Retsch SM 300), and stored in a covered plastic container at room temperature until further use.

Before conducting the hydrolysis experiments, 30 g of chopped and sieved feathers and 90 g of Milli-Q water were mixed and manually stirred until a homogeneous feather mass was formed.

2.2. Thermal Pressure Hydrolysis. For the hydrolysis experiment, the feather mass (5 g) and water (15 g) were loaded into stainless steel autoclaves (50 mL, PARR 5000 Multiple Reactor System, USA) equipped with magnetic stirring rods. The systems were heated to the target temperature in 10−12 min (PARR 4870 controller, Honeywell). Target hydrolysis temperatures ranged from 120 to 160 °C (5 °C as a step, the temperature was measured inside the feather mass). The hydrolysis reaction was performed for 10 and 30 min, corresponding to the four stages reported in our previous paper.[15] $t = 0$ was defined as the moment at which the reactor reached the target temperature. After the reaction, the reactor was placed in an ice bath for rapid cooling, after which the hydrolyzed feather mass was collected, weighed and dried overnight at 60 °C to a constant weight, manually milled and sieved (0.8 mm sieve), and stored in a glass vial at room temperature until further analysis.

2.3. FTIR Analysis. The samples (<0.8 mm) were dried in an oven at 60 °C overnight (Memmert, Germany). The FTIR measurement was conducted under laboratory conditions, for example, 20−25 °C. 1 mg of the protein sample and 200 mg of KBr (potassium bromide for IR spectroscopy, Merck) were ground using a mortar and pestle into a homogeneous powder and then pressed (9 tons, SPECAC, UK) into a clear pellet (diameter 10 mm). Spectra were recorded from 4000 to 400 cm^{-1} at a resolution of 4 cm^{-1}, and 64 scans without automatic CO_2 and H_2O compensation were averaged (Bruker, VERTEX 70, Germany). At least three independent measurements were conducted for each sample to fulfill the quality control, at least 95% similarity for the whole range (OPUS 7.5, Bruker, Germany). After atmospheric compensation and automatic baseline correction from 2200 to 900 cm^{-1} using OPUS 7.5 (Bruker, Germany), three spectra for each sample were averaged into one spectrum and normalized (0−1) using OriginPro (OriginLab Corp, USA). A principal component analysis (PCA) was conducted using OriginPro. The normalized spectra were curve-fitted using OriginPro, for example, range: 2000−1580 cm^{-1}, shape: Gaussian, flexible range for full width at half-maximum (FWHM): 27 to 80, repetition of curve fitting: $n = 10$. The average from 10 fitting results for each sample was calculated for evaluation. For simple molecules, IR absorption bands are usually assumed to be Lorentzian in shape. However, this assumption does not necessarily hold for larger, complex molecules such as proteins, and the shape of IR absorption bands arising from proteins is less than clear.[27] Therefore, we assume that the Gaussian distribution will be more suitable for feather keratins.

Calculation for the content of the ß-sheet is as follows

$$\text{Content of } \beta - \text{sheet}(\%) = (\text{area } 1635\ cm^{-1} + 1689\ cm^{-1})/\text{total integrated area}$$

Calculation for the content of 1700_{sum} is as follows

$$\text{Content of } 1700_{sum}(\%) = (\text{sum of area from } 2000\ cm^{-1} \text{ to } 1700\ cm^{-1})/\text{total integrated area}$$

There are two types of β-sheets present in the feathers, parallel and antiparallel, centered at 1635 and 1689 cm^{-1}, respectively. Therefore, the sum of both would represent the total number of β-sheets.

2.4. Chemical Analysis. Nitrogen contents were measured in duplicate using the DUMAS method according to ref[33]

https://doi.org/10.1021/acsomega.2c04216
ACS Omega 2022, 7, 39924−39930

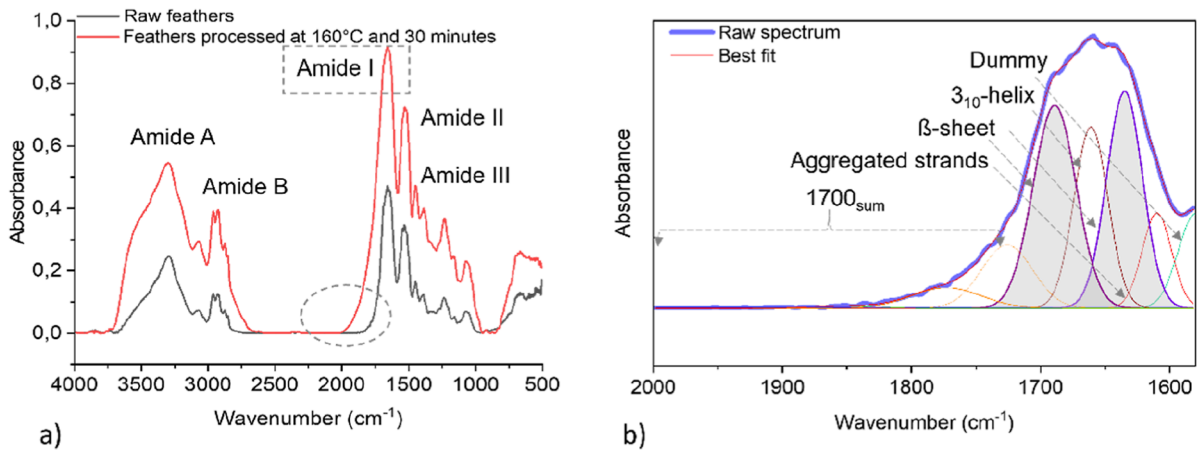

Figure 1. Typical examples of FTIR spectra from this study. (a) FTIR spectrum of raw feathers and feathers processed under maximum conditions (160 °C and 30 min). The rectangle shows amide I as the main curve fitting area, and the ellipse highlights the newly developed peaks caused by hydrolysis. (b) Enlarged image from 2100 to 1550 cm^{-1} for processed feathers (160 °C and 30 min).

(FlashEA 1112 Organic Elemental Analyzer, Thermo Scientific, USA). Samples were predried at 60 °C (Memmert, Germany). 10−15 mg of the sample was wrapped in an aluminum tin (nitrogen-free) and combusted at 900 °C in the presence of oxygen to convert all nitrogen to nitrogen oxides (NO_x). The released nitrogen oxides were separated from carbon dioxide and water before the nitrogen content was measured using a thermal conductivity detector (FlashEA 1112 Organic Elemental Analyzer, Thermo Scientific, USA).

The AEH was used to assess the reactivity (a measure for digestibility) of the partially hydrolyzed feathers. AEH is defined as the degree of degradation of processed feather protein by pepsin (77151, Sigma-Aldrich, NL) and pancreatin from porcine pancreas (P1750, Sigma-Aldrich, NL) according to a modified Boisen method.[34] The modification was performed using a Kuhner Climo-Shaker ISF1-X operated at 39 °C, 60 rpm for shaking, to create a constant atmosphere for pH adjustment and reaction as well as to perform multiple experiments in parallel. We used Formula 1 to calculate AEH.

$$AEH = N_{sample} - N_{residue} \quad (1)$$

whereAEH = availability for enzymatic hydrolysis in wt % of crude protein (wt % CP)N_{sample} = nitrogen content (sample) in wt % CP.$N_{residue}$ = nitrogen content (after digestion, undigested residue) in wt % CP.

2.5. Statistics. Statgraphics Centurion (Statgraphics Technologies, USA) was used to assess statistical relevance between the secondary structure and AEH with adjusted R^2 at three significance levels: $p < 0.001$, $p < 0.01$, and $p < 0.05$. Excel 2016 was used to calculate the standard deviation.

RESULTS AND DISCUSSION

Figure 1a shows a comparison between normalized FTIR spectra of an unhydrolyzed sample and one hydrolyzed at 160 °C for 30 min. New signals are clearly apparent after hydrolysis between 2000 and 1700 cm^{-1}. The assignment of relevant signals is summarized in Table 1. The most important area of focus is the 2000−1600 cm^{-1} range. Region 1700−1600 cm^{-1} represents the C═O vibrations in the amide bond (amide I) from which the secondary structure of the protein can be assigned.[27]Figure 1b shows one of the curve fitting results using eight Gaussian peaks to show the broadening of the curve from 2000 to 1700 cm^{-1}: Five peaks are present in the range from 1700 to 1580 cm^{-1}, whereas three peaks are present in the range from 2000 to 1700 cm^{-1}.[27] These latter three peaks, that is, 1700_{sum}, represent C═O stretching;[35] they are included to obtain a good fit and are therefore relevant for assessing structural changes. The curve fitting (n = 10) showed consistent results with a small standard deviation from 0 to 0.43 (for details, see the Supporting Information).

Table 1. Assignment of Relevant FTIR Signals for Analysis of Unhydrolyzed Feathers and Hydrolyzed Feathers

wavenumber, cm^{-1}	assignment	vibration
2000−1700		C═O stretching vibration
1700−1600	amide I, secondary structure	C═O stretching vibration (80%), C−N stretching (about 10%), and N−H bending (about 10%)
1610	aggregated strands[27] /side chain amino group[36,37]	
1635	parallel ß-pleated sheet	
1661	3_{10}-helix[27] /α-helix/turns[7,26]	
1689	antiparallel ß-pleated sheet	
1583	amide II	out-of-phase combination of N−H bending (60%)

Latent variable methods such as PCA have become standard in spectroscopy. One of the advantages of latent variable methods is that they reveal the underlying dimensionality of the system at study. The FTIR peaks are not independent, and even if there are many peaks, the number of underlying phenomena that vary is often low. PCA was applied to find difference in samples and potential dimensionality of the system.[38]Figure 2 shows a clear trend with increased processing temperature, for example, from B009 (raw feathers) to B16 (processed at 160 °C).

Feathers have a high ß-sheet content (>75%) which is related to their low AEH;[6] it can thus be expected that a change in the ß-sheet content is related to their digestibility. We established the ß-sheet content as a function of temperature and time during TPH by FTIR spectroscopy and investigated the relation between the ß-sheet content and AEH (Figure 3). Figure 3a shows the ß-sheet content (sum of the area of IR bands at 1635 and 1689 cm^{-1}) at different temperatures (120−160 °C) and after different processing

https://doi.org/10.1021/acsomega.2c04216
ACS Omega 2022, 7, 39924−39930

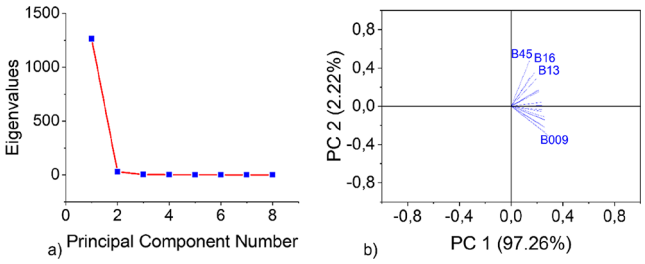

Figure 2. PCA. (a) Eigenvalues. (b) Loading plot.

times (10 and 30 min). Figure 3b shows the relationship between the ß-sheet content and AEH as inferred from FTIR spectra.

For temperatures up to 140 °C, the ß-sheet content did not change as a function of temperature, and only above 140 °C did the ß-sheet content decrease (Figure 3a). It should be noted that in an earlier work,[15] the digestibility of processed feathers only significantly increased above 140 °C, indicating a relationship between the ß-sheet content and AEH. Figure 3b shows that this increased AEH is related to the ß-sheet content. As the ß-sheet is the focus of this study, the correlation between other structures and AEH is shown in the Supporting Information. In addition, time (10 or 30 min) only had a minor influence on the ß-sheet content and thus on AEH for the tested duration of hydrolysis.

In the temperature range of 120−140 °C, no change in the ß-sheet structure was observed. This is in line with the literature which indicates that at these low temperatures, only free and weakly bound water is released,[39] without a change in secondary and primary structures.[40] In an earlier work, Goerner-Hu et al. indicated that below 140 °C, AEH did increase but only to a minor extent.[15] This can be attributed to the breaking of disulfide bonds in the feathers, which has been reported to occur around 100 °C.[41] Above 140 °C, AEH increased significantly (Figure 3b). This is related to a decrease in the content of ß-sheets which then leads to feather protein uncoiling.[40] As a result, the feather protein structure opens and becomes accessible for enzymatic hydrolysis.

We only investigated the role of the total ß-sheet structure (i.e., we combined the areas of the peaks at 1635 and 1689 cm^{-1}) as a function of TPH treatment. Both components of the ß-sheet, that is, the parallel ß-sheet at 1635 cm^{-1} and the antiparallel ß-sheet at 1689 cm^{-1}, showed temperature dependences (Figures 4a and 5a). Both changes of parallel and antiparallel ß-sheets are related to AEH (Figures 4b and 5b).

Using the FTIR approach, we show that the total ß-sheet content decreases during TPH, which is related to the AEH; FTIR is a simple method to predict AEH. We also observed the development of new peaks after hydrolysis in the 1700−2000 cm^{-1} range in addition to changes in the other peaks [S2−S4, Supporting Information, for the relation with the other components, i.e., at 1585 cm^{-1} (amide II, Table 1), at 1610 cm^{-1} (aggregated strands/side chain amino group, Table 1), and at 1660 cm^{-1} (3_{10}-helix/ß−turn, Table 1)]. Figure 6a shows a clear relation between the ß-sheet content and the content of the 1700_{sum} peaks. A linear relationship can be clearly observed between 1700_{sum} and the AEH (Figure 6b). Therefore, the 1700_{sum} peak is an efficient indicator for the AEH of processed feathers. An advantage of the 1700_{sum} band is that it is located outside the amide I area and therefore overlaps less with other signals.[36] Therefore, changes can be more clearly observed.

Currently, the physical/chemical meaning of 1700_{sum} remains an enigma. However, it is known that hydrogen bonding changes the secondary structure which IR spectroscopy is uniquely sensitive to.[42,43] The structural change during TPH may be due to a rearrangement of hydrogen bonds in the secondary structure caused by their different thermal stabilities.[31,32,44] Also, the peaks from 2000 to 1700 cm^{-1} mainly correspond to the C═O stretching vibration which is sensitive to H-bonding after formation of strong hydrogen bonds.[35,36]

In summary, the results confirm that the secondary structure is an essential factor affecting AEH of feathers. Interestingly, not all ß-sheets changed during TPH (60 to 40%) (S1, Supporting Information). The partial change in the total ß-sheet shows the different thermal stabilities of hydrogen bonds in the feather structure and, more importantly, that only a part is responsible for the change in AEH.

4. CONCLUSIONS

This study investigated the use of FTIR spectroscopy to assess the structural change in feathers and its impact on AEH during TPH. The content of the total ß-sheet in the feathers decreased with increasing temperature and duration, while the peaks from 2000 to 1700 cm^{-1} (1700_{sum}) increased. During heat treatment, hydrogen bonds which held the ß-sheet structure were rearranged due to their different thermal stabilities, changing the spatial structure in the native feathers. This led to the amino acids hidden in the secondary structure

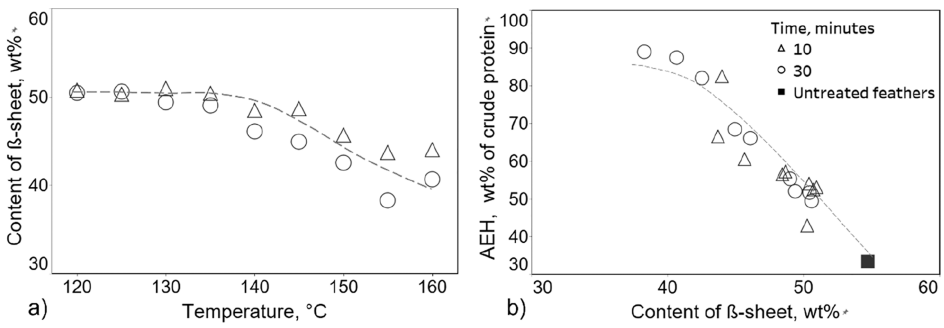

Figure 3. Relationship between the process conditions (temperature and time), total ß-sheet content, and AEH. (a) Significance for the temperature and total ß-sheet content at different times, $p < 0.01$, $R^2 = 0.95$ at 10 min and $p < 0.0001$, $R^2 = 0.96$ at 30 min. (b) Significance for the total ß-sheet content and AEH, $p < 0.0001$, $R^2 = 0.92$. Solid square: raw feathers.

https://doi.org/10.1021/acsomega.2c04216
ACS Omega 2022, 7, 39924−39930

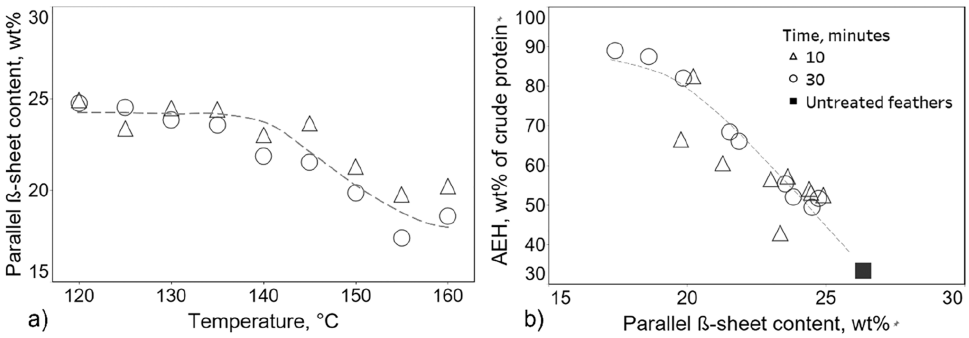

Figure 4. Relationship between the process conditions (temperature and time), parallel ß-sheet content, and AEH. (a) Significance for the temperature and parallel ß-sheet content at different times, $p < 0.05$, $R^2 = 0.85$ at 10 min and $p < 0.01$, $R^2 = 0.95$ at 30 min. (b) Significance for the parallel ß-sheet content and AEH, $p < 0.0001$, $R^2 = 0.86$. Solid square: raw feathers.

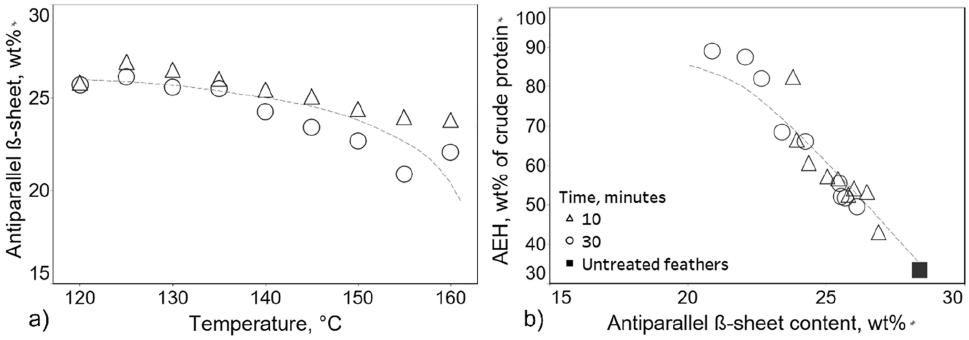

Figure 5. Relationship between the process conditions (temperature and time), antiparallel ß-sheet content, and AEH. (a) Significance for the temperature and antiparallel ß-sheet content at different times, $p < 0.0001$, $R^2 = 0.97$ at 10 min and $p < 0.0001$, $R^2 = 0.96$ at 30 min. (b) Significance for the antiparallel ß-sheet content and AEH, $p < 0.0001$, $R^2 = 0.92$. Solid square: raw feathers.

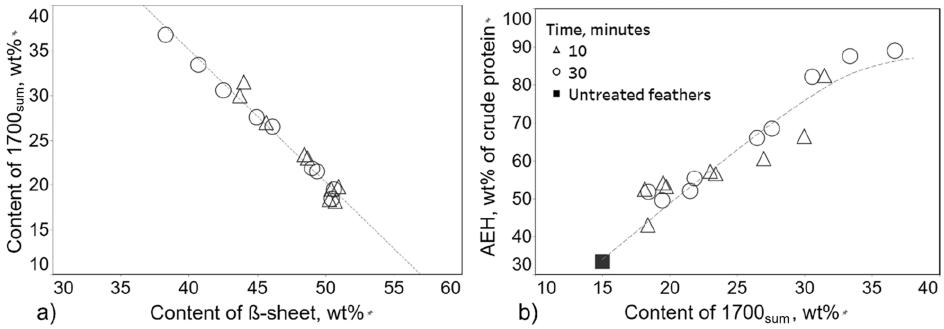

Figure 6. (a) Relationship between the total ß-sheet content and 1700_{sum}, $p < 0.0001$, $R^2 = 0.97$. (b) Relationship between the content of 1700_{sum} and AEH, $p < 0.0001$, $R^2 = 0.92$; solid square: raw feathers.

becoming accessible to digestive enzymes, resulting in increased AEH. In conclusion, the FTIR method is suitable to detect the molecular structure change induced by heat. The method in the present study simplified the use of FTIR spectroscopy to evaluate the processed feather proteins. Because the structural change is related to AEH, it is possible to get a quick overview of AEH during the production based on the FTIR spectrum. Therefore, FTIR analysis has a good potential for gathering preliminary information about AEH before a thorough chemical analysis and can even be an alternative to chemical analysis..

■ ASSOCIATED CONTENT

Supporting Information

The Supporting Information is available free of charge at https://pubs.acs.org/doi/10.1021/acsomega.2c04216.

Average content and deviation of structure; relationship between the process conditions, content at 1580−1590 cm^{-1}, and AEH; relationship between the process conditions, content at 1609−1611 cm^{-1}, and AEH; and relationship between the process conditions, content at 1660−1662 cm^{-1}, and AEH (PDF)

■ AUTHOR INFORMATION

Corresponding Author

Johannes H. Bitter − *Biobased Chemistry and Technology, Wageningen University & Research, 6708WG Wageningen, Netherlands;* orcid.org/0000-0002-4273-9968; Phone: +31 317 480303; Email: harry.bitter@wur.nl

https://doi.org/10.1021/acsomega.2c04216
ACS Omega 2022, 7, 39924−39930

Authors

Xinhua Windt − *Biobased Chemistry and Technology, Wageningen University & Research, 6708WG Wageningen, Netherlands; Saria International GmbH, 59379 Selm, Germany*

Elinor L. Scott − *Biobased Chemistry and Technology, Wageningen University & Research, 6708WG Wageningen, Netherlands*

Thorsten Seeger − *Saria International GmbH, 59379 Selm, Germany*

Oliver Schneider − *Saria International GmbH, 59379 Selm, Germany*

Akbar Asadi Tashvigh − *Biobased Chemistry and Technology, Wageningen University & Research, 6708WG Wageningen, Netherlands;* orcid.org/0000-0003-0454-0314

Complete contact information is available at: https://pubs.acs.org/10.1021/acsomega.2c04216

Funding

This work was financially supported by Saria International GmbH.

Notes

The authors declare no competing financial interest.

■ ACKNOWLEDGMENTS

The authors wish to thank Dr. Lars Kiewidt for his valuable input.

■ ABBREVIATIONS USED

AEH, availability for enzymatic hydrolysis; ß-sheet, ß-pleated sheet; TPH, thermal pressure hydrolysis; wt % CP, wt % of crude protein; 1700_{sum}, sum of peaks from 2000 to 1700 cm^{-1}; R^2, adjusted R^2 (coefficient of determination)

■ REFERENCES

(1) Marquer, P.; Rabade, T.; Forti, R.*Meat production statistics*, 18th June 2018. Date accessed November 19th, 2018, ed.; eurostat:. http://ec.europa.eu/eurostat/statistics-explained/index.php?title=Meat_production_statistics.

(2) Lasekan, A.; Abu Bakar, F. A.; Hashim, D. Potential of chicken by-products as sources of useful biological resources. *Waste Manage* **2013**, *33*, 552−565.

(3) Bureau, D. P.The Nutritive Value of Processed Animal Proteins to Different Aquaculture Species*EFPRA, FNRL Fish Nutrition Research*; Lab University of Guelph: Prague, 2013.

(4) Papadopoulos, M. C. Effect of processing on high-protein feedstuffs: A review. *Biol. Wastes* **1989**, *29*, 123−138.

(5) Grazziotin, A.; Pimentel, F. A.; de Jong, E. V.; Brandelli, A. Nutritional improvement of feather protein by treatment with microbial keratinase. *Anim. Feed Sci. Technol.* **2006**, *126*, 135−144.

(6) Yu, P. Protein secondary structures (a-helix and b-sheet) at a cellular level and protein fractions in relation to rumen degradation behaviours of protein: a new approach. *Br. J. Nutr.* **2005**, *94*, 655−665.

(7) Güler, G.; Dzafic, E.; Vorob'ev, M. M.; Vogel, V.; Mäntele, W. Real time observation of proteolysis with Fourier transform infrared (FT-IR) and UV-circular dichroism spectroscopy: Watching a protease eat a protein. *Spectrochim. Acta, Part A* **2011**, *79*, 104−111.

(8) Wang, B.; Yang, W.; McKittrick, J.; Meyers, M. A. Keratin: Structure, mechanical properties, occurrence in biological organisms, and efforts at bioinspiration. *Prog. Mater. Sci.* **2016**, *76*, 229−318.

(9) Meeker, D. L.; Meisinger, J. L. Companion aminals symposium: Rendered ingredients significantly influence sustainability, quality, and safety of pet food1. *J. Anim. Sci.* **2015**, *93*, 835−847.

(10) Callegaro, K.; Brandelli, A.; Daroit, D. J. Beyond plucking: Feathers bioprocessing into valuable protein hydrolysates. *Waste Manage* **2019**, *95*, 399−415.

(11) Barone, J. R.; Schmidt, W. F.; Gregoire, N. T. Extrusion of Feather Keratin. *J. Appl. Polym. Sci.* **2005**, *100*, 1432−1442.

(12) Coward-Kelly, G.; Chang, V. S.; Agbogbo, F. K.; Holtzapple, M. T. Lime treatment of keratinous materials for the generation of highly digestible animal feed: 1. Chicken feathers. *Bioresour. Technol.* **2006**, *97*, 1337−1343.

(13) Jin, H.-S.; Park, S. Y.; Kim, J.-Y.; Lee, J.-E.; Lee, H.-S.; Kang, N. J.; Lee, D.-W. Fluorescence-based Quantification of Bioactive Keratin Peptides from Feathers for Optimizing Large-scale Anaerobic Fermentation and Purification. *Biotechnol. Bioprocess Eng.* **2019**, *24*, 240−249.

(14) Meeker, D. L.; Hamilton, C. R.*An overview of the rendering industry*; National Renderers Association: Alexandria, USA, 2006.

(15) Goerner-Hu, X.; Scott, E. L.; Seeger, T.; Schneider, O.; Bitter, J. H. Reaction stages of feather hydrolysis: Factors that influence availability for enzymatic hydrolysis and cystine conservation during thermal pressure hydrolysis. *Biotechnol. Bioprocess Eng.* **2020**, *25*, 749−757.

(16) Boisen, S. In vitro analyses for predicting standardised ileal digestibility of protein and amino acids in actual batches of feedstuffs and diets for pigs. *Livestock Science* **2007**, *109*, 182−185.

(17) Zhou, D.; Chen, X.-P.; Liang, J.-Z.; Wei, X.-J.; Wu, C.-H.; Li, W.-H.; Wang, L.-L. High-Temperature Stability and Pyrolysis Kinetics and Mechanism of Bio-Based and Petro-Based Resins Using TG−FTIR/MS. *Ind. Eng. Chem. Res.* **2021**, *60*, 13774−13789.

(18) Xing, Y.-X.; Wang, Y.-R.; Huang, J.-C.; Fei, Z.-Y.; Liu, Q.; Chen, X.; Cui, M.-F.; Qiao, X. Study on the Mechanism and Kinetics of Waste Polypropylene Cracking Oxidation over the Mn2O3/HY Catalyst by TG−MS and In Situ FTIR. *Ind. Eng. Chem. Res.* **2020**, *59*, 16569−16578.

(19) Kong, J.; Yu, S. Fourier Transform Infrared Spectroscopic Analysis of Protein Secondary Structures. *Acta Biochim Biophys Sin* **2007**, *39*, 549−559.

(20) Bertram, H. C.; Kohler, A.; Böcker, U.; Ofstad, R.; Andersen, H. J. Heat-Induced Changes in Myofibrillar Protein Structures and Myowater of Two Pork Qualities. A Combined FT-IR Spectroscopy and Low-Field NMR Relaxometry Study. *J. Agric. Food Chem.* **2006**, *54*, 1740−1746.

(21) Bai, M.; Qin, G.; Sun, Z.; Long, G. Relationship between molecular structure characteristics of feed proteins and protein in vitro digestibility and solubility. *Asian-Australas J Anim Sci* **2016**, *29*, 1159−65.

(22) Güler, G.; Vorob'ev, M. M.; Vogel, V.; Mäntele, W. Proteolytically-induced changes of secondary structural protein conformation of bovine serum albumin monitored by Fourier transform infrared (FT-IR) and UV-circular dichroism spectroscopy. *Spectrochim. Acta, Part A* **2016**, *161*, 8−18.

(23) Yu, P.; McKinnon, J. J.; Christensen, C. R.; Christensen, D. A. Using Synchrotron-Based FTIR Microspectroscopy To Reveal Chemical Features of Feather Protein Secondary Structure: Comparison with Other Feed Protein Sources. *J. Agric. Food Chem.* **2004b**, *52*, 7353−7361.

(24) Cardamone, J. M. Investigating the microstructure of keratin extracted from wool: Peptide sequence (MALDI-TOF/TOF) and protein conformation (FTIR). *J. Mol. Struct.* **2010**, *969*, 97−105.

(25) Takahashi, K.; Yamamoto, H.; Yokote, Y.; Hattori, M. Thermal Behavior of Fowl Feather Keratin. *Biosci., Biotechnol., Biochem.* **2004**, *68*, 1875−1881.

(26) Barth, A. Infrared spectroscopy of proteins. *Biochim. Biophys. Acta* **2007**, *1767*, 1073−1101.

(27) Jackson, M.; Mantsch, H. H. The use and misuse of FTIR sepctroscopy in the determination of protein structure. *Crit. Rev. Biochem. Mol. Biol.* **1995**, *30*, 95−120.

(28) Hamminga, G. M.; Mul, G.; Moulijn, J. A. Real-time in situATR-FTIR analysis ofthe liquid phase hydrogenation of γ-

butyrolactone over Cu-ZnO catalysts:A mechanistic study by varying lactone ring size. *Chem. Eng. Sci.* **2004**, *59*, 5479−5485.
(29) Wong, S.-W.; Georgakis, C.; Botsaris, G. D.; Saranteas, K.; Bakale, R. Online Estimation and Monitoring of Diastereomeric Resolution Using FBRM, ATR-FTIR, and Raman Spectroscopy. *Ind. Eng. Chem. Res.* **2008**, *47*, 5576−5584.
(30) Khanlari, S.; Dubé, M. A. Reaction Monitoring of in Situ Formation of Poly(sodium acrylate)Based Nanocomposites Using ATR-FTIR Spectroscopy. *Ind. Eng. Chem. Res.* **2015**, *54*, 5598−5603.
(31) Guo, L.-H.; Sato, H.; Hashimoto, T.; Ozaki, Y. FTIR Study on Hydrogen-Bonding Interactions in Biodegradable Polymer Blends of Poly(3-hydroxybutyrate) and Poly(4-vinylphenol). *Macromolecules* **2010**, *43*, 3897−3902.
(32) Kuo, S.-W.; Chen, C.-J. Using Hydrogen-Bonding Interactions To Control the Peptide Secondary Structures and Miscibility Behavior of Poly(L-glutamate)s with Phenolic Resin. *Macromolecules* **2011**, *44*, 7315−7326.
(33) Jung, S.; Rickert, D. A.; Deak, N. A.; Aldin, E. D.; Recknor, J.; Johnson, L. A.; Murphy, P. Comparison of Kjeldahl and Dumas Methods for Determining Protein Contents of Soybean Products. *J. Am. Oil Chem. Soc.* **2003**, *80*, 1169−1173.
(34) Boisen, S.; Fernández, J. A. Prediction of the apparent ileal digestibility of protein and amino acids in feedstuffs and feed mixtures for pigs by in vitro analyses. *Anim. Feed Sci. Technol.* **1995**, *51*, 29−43.
(35) OChemOnline*Infrared Spectroscopy Absorption Table 25*, Sep, 2019: LibreTexts libraries. https://chem.libretexts.org/Bookshelves/Ancillary_Materials/Reference/Reference_Tables/Spectroscopic_Parameters/Infrared_Spectroscopy_Absorption_Table.
(36) Barth, A. The infrared absorption of amino acid side chains. *Prog. Biophys. Mol. Biol.* **2000**, *74*, 141−173.
(37) Bhattacharjee, C.; Saha, S.; Biswas, A.; Kundu, M.; Ghosh, L.; Das, K. P. Structural Changes of b-Lactoglobulin during Thermal Unfolding and Refolding − An FT-IR and Circular Dichroism Study. *The Protein Journal* **2005**, *24*, 27−35.
(38) Matwijczuk, A.; Oniszczuk, T.; Chruściel, E.; Kocira, A.; Niemczynowicz, A.; Wójtowicz, A.; Combrzyński, M.; Wiącek, D. Use of FTIR Spectroscopy and Chemometrics with Respect to Storage Conditions of Moldavian Dragonhead Oil. *Sustainability* **2019**, *11*, 1−16.
(39) Milczarek, P.; Zielinski, M.; Garcia, M. L. The mechanism and stability of thermal transitions in hair keratin. *Colloid Polym. Sci.* **1992**, *270*, 1106−1115.
(40) Adler-Nissen, J.*A Review of Food Protein Hydrolysis - General Issues*; Elsevier applied science publishers LTD, 1986, p 31.
(41) Mackiewicz, M.; Romanski, J.; Drozd, E.; Gruber-Bzura, B.; Fiedor, P.; Stojek, Z.; Karbarz, M. Nanohydrogel with N,N0-bis(acryloyl)cystine crosslinker for high drug loading. *Int. J. Pharm.: X* **2017**, *523*, 336−342.
(42) Murayama, K.; Tomida, M. Heat-Induced Secondary Structure and Conformation Change of Bovine SerumAlbumin Investigated by Fourier Transform Infrared Spectroscopy. *Biochemistry* **2004**, *43*, 11526−11532.
(43) Chen, S.; Xu, C.-Q.; Mao, L.-K.; Liu, F.-G.; Sun, C.-X.; Dai, L.; Gao, Y.-X. Fabrication and characterization of binary composite nanoparticles between zein and shellac by anti-solvent co-precipitation. *Food Bioprod. Process.* **2018**, *107*, 88−96.
(44) Ragone, P. Hydrogen-bonding classes in proteins and theircontribution to the unfolding reaction. *Protein Sci.* **2001**, *10*, 2075−2082.

https://doi.org/10.1021/acsomega.2c04216
ACS Omega 2022, 7, 39924−39930